

SCIENTIFIC REPORTS



OPEN

Epigenetic silencing of miR-19a-3p by cold atmospheric plasma contributes to proliferation inhibition of the MCF-7 breast cancer cell

Received: 26 April 2016

Accepted: 28 June 2016

Published: 21 July 2016

Seungyeon Lee^{1,*}, Hyunkyung Lee^{1,*}, Hansol Bae¹, Eun H. Choi² & Sun Jung Kim¹

Cold atmospheric plasma (CAP) has been proposed as a useful cancer treatment option after showing higher induction of cell death in cancer cells than in normal cells. Although a few studies have contributed to elucidating the molecular mechanism by which CAP differentially inhibits cancer cell proliferation, no results are yet to be reported related to microRNA (miR). In this study, miR-19a-3p (miR-19a) was identified as a mediator of the cell proliferation-inhibitory effect of CAP in the MCF-7 breast cancer cell. CAP treatment of MCF-7 induced hypermethylation at the promoter CpG sites and downregulation of miR-19a, which was known as an oncomiR. The overexpression of miR-19a in MCF-7 increased cell proliferation, and CAP deteriorated the effect. The target genes of miR-19a, such as ABCA1 and PTEN, that had been suppressed by miR recovered their expression through CAP treatment. In addition, an inhibitor of reactive oxygen species that is produced by CAP suppressed the effect of CAP on cell proliferation. Taken together, the present study, to the best of authors' knowledge, is the first to identify the involvement of a miR, which is dysregulated by the CAP and results in the anti-proliferation effect of CAP on cancer cells.

Cold atmospheric pressure plasma (CAP) is ionized media that mainly contains reactive oxygen species (ROS) and reactive nitrogen species (RNS)¹. Ever since CAP was successfully produced in cold conditions, it has been given attention for medical applications, especially cancer treatment². In fact, CAP has been widely proven to be able to differentially inhibit the growth of cancer cells compared with their normal counterpart in various cancer types. For example, when *in vitro*-cultured cancer cells, such as melanoma³, breast cancer⁴, and lung cancer cells⁵, were exposed to CAP, the cells showed growth retardation, increased double-strand breaks (DSB), and increased apoptosis. The CAP also worked effectively in *in vivo* animal models to treat xenografted cancer and promote wound healing. In detail, ovarian cancer cells xenografted into a mouse underwent cell death from the injection of CAP-activated medium⁶. In another study, CAP led to the successful skin wound healing of mice⁷. Clinically, patients suffering from chronic leg ulcers were treated in a clinically controlled monocentric trial with CAP⁸. The immediate antimicrobial effects of the CAP were almost comparable to octenidine treatment without any signs of cytotoxicity.

The molecular mechanism of how CAP changes cellular phenomena is being elucidated. So far, the main casts of CAP related to biological function are believed to be reactive nitrogen species (RNS) and reactive oxygen species (ROS)⁹. For ROS, its production and effect on cancer cells have been documented in many studies^{10–12}. The ROS was shown to easily penetrate the cell membrane and diffuse to cytosol¹³, where it modulates or transduces diverse signaling, eventually leading to the regulation of gene expression. This phenomenon was supported in a series of studies that explained the same change of gene expression or cellular activity by CAP and ROS. An example is the observation of the dysregulation of TGF- α , VEGF¹⁴, and CDH1¹⁵ by either CAP or ROS. On the other hand, it seems that CAP also has unique regulatory pathways because in many cases CAP resulted in

¹Department of Life Science, Dongguk University-Seoul, Goyang, Korea. ²Plasma Bioscience Research Center, Kwangwoon University, Seoul, Korea. *These authors contributed equally to this work. Correspondence and requests for materials should be addressed to S.J.K. (email: sunjungk@dongguk.edu)

Symbol	Accession no.	Description	Delta mean	Fold change	Target ID
MIR219A1	NR_029633	microRNA 219a-1	0.1854	2.1735	cg14363494
MIR2117	NR_031751	microRNA 2117	0.1842	2.1397	cg03184776
MIR449C	NR_031572	microRNA 449c	0.1750	1.5578	cg14079131
MIR18A	NR_029488	microRNA 18a	0.1717	2.3564	cg07235355
MIR17	NR_029487	microRNA 17	0.1717	2.3564	cg07235355
MIR19A	NR_029489	miRNA 19a	0.1717	2.3564	cg07235355
MIR4258	NR_036212	microRNA 4258	0.1687	1.9979	cg06418219
MIR5692A1	NR_049875	microRNA 5692a-1	0.1667	2.6457	cg03068446
MIR615	NR_030753	microRNA 615	0.1570	1.6089	cg14644523
MIR484	NR_030159	microRNA 484	0.1536	1.6919	cg06397424
MIR3143	NR_036096	microRNA 3143	0.1532	1.6837	cg21201844
MIRLET71	NR_029661	microRNA let-7i	0.1528	1.5182	cg06162516
MIR5189	NR_049821	microRNA 5189	-0.1575	-1.2741	cg02383666
MIR29C	NR_029832	miRNA 29c	-0.1737	-1.2691	cg00823526
MIR29B2*	NR_029518	microRNA 29b-2	-0.1737	-1.2691	cg00823526
			-0.1872	-1.2709	cg22525895
MIR103A2	NR_029519	microRNA 103a-2	-0.1865	-1.3055	cg12617066
MIR103B2	NR_031722	microRNA 103b-2	-0.1865	-1.3055	cg12617066

Table 1. MicroRNAs displaying differential methylation in MCF-7 cells exposed to CAP. *MIR29B2 contains two CpG sites with differential methylation.

non-overlapping pathways with the reactive species. For example, in cervical cancer cells, the MAPK pathway was suppressed through decreasing MMP9 by CAP¹⁶. In another study, p53 and p21 were dysregulated by CAP¹⁷, which has not been observed in cells treated with reactive species.

CAP can induce a genetic change of DNA in the nucleus by producing a double-strand break (DSB). CAP-treated lung cancer cells showed DSB, thereby leading to apoptosis⁵. Whether CAP can directly induce DSB in the cell is yet to be elucidated, although it was shown to induce DSB in leucocytes embedded in agarose¹⁸. Other than DSB, little is known about genetic changes of DNA at a base level, such as the mutation of nucleotides. As an alternative explanation for the diverse changes of gene expression as well as cellular activities by CAP, epigenetic factors, such as CpG methylation, miR, and histone modification, have emerged^{19,20}. Recently, in our previous study, a genome-wide methylation change by CAP in breast cancer cells was examined, and many cancer-related genes were revealed to have undergone methylation changes at their promoter CpG sites²¹.

In this study, we screened a collection of miRs to identify specific miRs that underwent a methylation change at the promoter CpG sites and thereby showed the alteration of gene expression by CAP. MiR-19a-3p (miR-19a) was found to have a good association between the methylation and expression level. To prove that miR-19a is truly regulated by CAP, the expression change for a few target genes of the miR were also examined. In addition, an ROS inhibitor was used to determine whether the effect of CAP on the expression of miR and target genes could be ablated.

Results

CAP induced hypermethylation and downregulation of miR-19a in MCF-7. In a previous study, we carried out a genome-wide methylation chip analysis and identified a group of genes for which the methylation status was significantly altered by CAP²¹. In the list of affected genes, also included were the promoter CpG sites of miRs. The array covered 42 noncoding RNAs, including 17 miRs (Table 1), and 25 long noncoding RNAs (Supplementary Table S1) showed a significant methylation change, satisfying our screening criteria (β -values equal to or greater than 0.15). An Ingenuity pathway analysis with the 42 non-coding RNAs identified “Cancer, Organismal Injury and Abnormalities, Gastrointestinal Disease” as the top interaction network (Fig. 1). Notably, a few miRs, including miR-19a, which have been known to be involved in carcinogenesis showed altered methylation by CAP (Fig. 2A). For example, miR-484 is known as an oncomir in breast cancer²², which is hypermethylated by CAP ($\Delta\beta = 0.153$). Additionally, miR-17, which is known as an oncomir in hepatocellular carcinoma²³, is hypermethylated ($\Delta\beta = 0.172$). Meanwhile, miR-29 ($\Delta\beta = -0.174$) and miR-103 ($\Delta\beta = -0.187$), which have tumor-suppressive activity in prostate cancer^{24,25}, are hypomethylated.

In further studies, we paid attention to the oncogenic miRs (called oncomiRs). We hypothesized that the hypermethylation of the oncomiRs by CAP would accompany the downregulation of gene expression, eventually resulting in a decrease of cell proliferation. Among the 17 miRs, miR-19a, miR-17²³, and miR-18a²⁶ were identified as oncomiRs from the PubMed database search. RT-PCR analysis revealed that only miR-19a showed a significant downregulation of expression, with an approximately 40% decrease by CAP treatment (Fig. 2B,C). MiR-19a, therefore, was selected to further examine its role in mediating the effect of CAP on the inhibition of cancer cell proliferation.

CAP deteriorated cell-proliferative effect of miR-19a in MCF-7. MiR-19a has been known to stimulate cell proliferation in a few cancers, including gastric and pancreatic cancer, where the miR is upregulated,

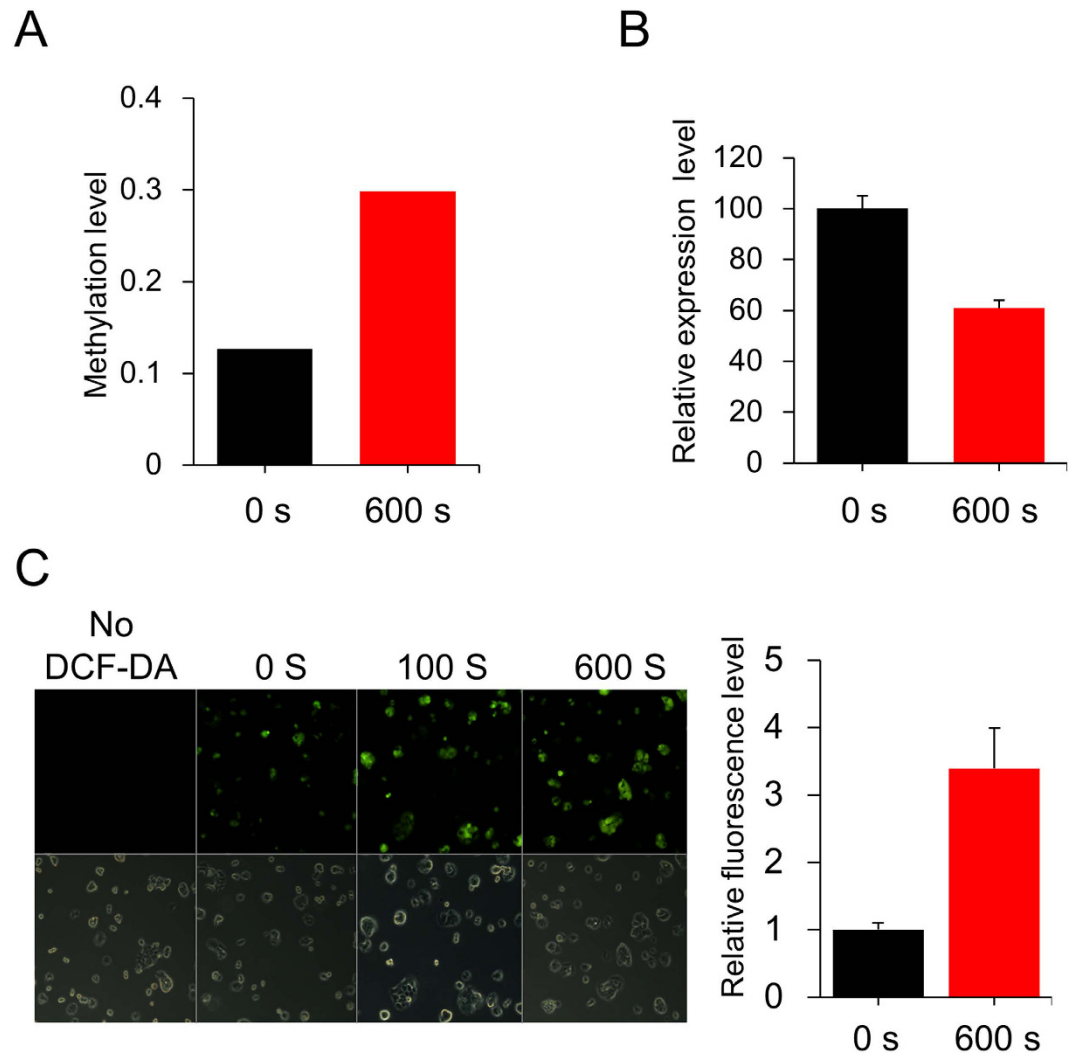


Figure 2. Induction of hypermethylation and downregulation of miR-19a in MCF-7 by CAP. (A) Methylation level of CpGs at the promoter of miR-19a after CAP treatment. The data are from methylation microarray analysis of MCF-7 treated with CAP. (B) Real-time RT-PCR analysis of miR-19a (Mean \pm SE of three replicates). (C) Fluorescence microscopic images of the MCF-7 cell after treating the cell with CAP for 0, 100, and 600 s following addition of DCF-DA. The bottom panel shows images from bright-field microscopy. The bar graph to the right shows quantification of fluorescence intensity for 600 s (Mean \pm SE of three replicates).

expression. For example, the activation of the MAPK and p53 signaling pathways was found as a result of CAP exposure in the non-small-cell lung cancer A549 cell, resulting in changes of expression for MEKK, GADD, FOS, and JUN³⁵. The MAPK signaling pathways seem to be a major CAP target because they appeared in other cell types, including immune cell lines (Jurkat and THP-1)³⁶ and melanoma cells³⁷. In another study, CAP-induced ROS disturbed the mitochondrial-nuclear network in the A549 lung cancer cell through a caspase-independent apoptotic pathway by downregulating the anti-apoptotic protein Bcl2, but by no activation of caspase 3/7³².

Another possible explanation is the regulation of methylation status at the CpG sites of the promoter, as shown for the miR-19a in this study. In our previous study, CAP was also able to change the methylation status at the promoter CpG sites of a set of coding genes that were involved in cell proliferation²¹. Further future studies should focus on elucidating how CAP regulates factors, mainly methyltransferase, to adjust the methylation level.

It is impressive that CAP suppressed the pro-proliferative effect of the oncomiR by upregulating its target genes, such as ABCA1, PTEN, HBP1, and GJA1, when CAP was used to treat the miR-19a-transfected cell. Interestingly, ABCA1 and PTEN are targets of TGF- β , and their downregulation is associated with poor prognosis in various cancers, including ovarian³⁸ and breast cancer^{39,40}. HBP1 is a tumor suppressor whose expression is lower in breast tumors targeted by the PI α /FOXO pathway⁴¹. GJA1 (also known as Connexin-43) is a connexin family protein and forms the gap junction. It is expressed primarily in myoepithelial cells and inhibits mammary gland tumor metastasis⁴². These characteristics of target genes as tumor suppressors in various cancer types support the suppressive effect of CAP against miR-19a.

A wide range of CAP treatment times have been applied to cells and successfully resulted in cell death. The treatment of head and neck squamous cancer cells with a surface micro-discharging (SMD) CAP for 30 s–180 s

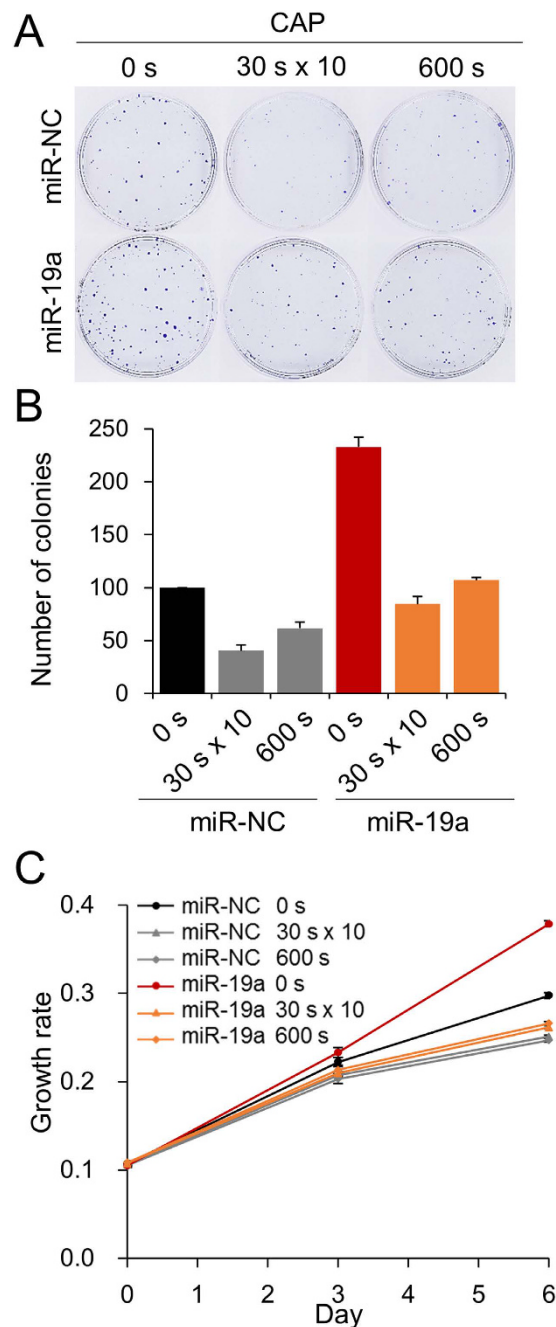


Figure 3. CAP suppresses cell proliferation driven by miR-19a. The effect of CAP on miR-19a-transfected MCF-7 was examined by colony formation assay (A). Transfected cells were treated with CAP by 600 s or 10 times for 30 sec scheme. The number of colonies was counted using ImageJ⁴⁷ and indicated as a bar graph (B). The effect of CAP was also analyzed by dye-based cell proliferation assay (C). MiR-transfected cells were treated with CAP and assayed at day 0, 3, and 6. MiR-NC; control miR. All the assays were performed in triplicates, and the result is depicted as Mean \pm SE.

decreased the cell viability in all treatment times⁴³. When Hattori *et al.* pre-treated the culture medium for 1–5 min and added it to pancreatic cancer cells, the cell growth of all the treated groups was inhibited⁴⁴.

In this study, two different strength conditions of CAP were applied to cells: a single shot of 600 s and 10 times for 30 s with a one-hour interval. Both the adopted strength ranges of CAP have shown the same cellular phenomena in terms of cell proliferation and apoptosis, although the 10 times for 30 s shot showed stronger cell proliferation inhibition. Furthermore, the target genes also showed higher expression changes in the case of the 10 times for 30 s shot. So far, a few signals of DBD CAP with different powers and duration times have been successfully applied to cancer cells to induce cell death with a specific gene expression change. Our study and previous studies suggest the possibility of designing a specific CAP strength that can modulate specific cellular activity and gene expression.

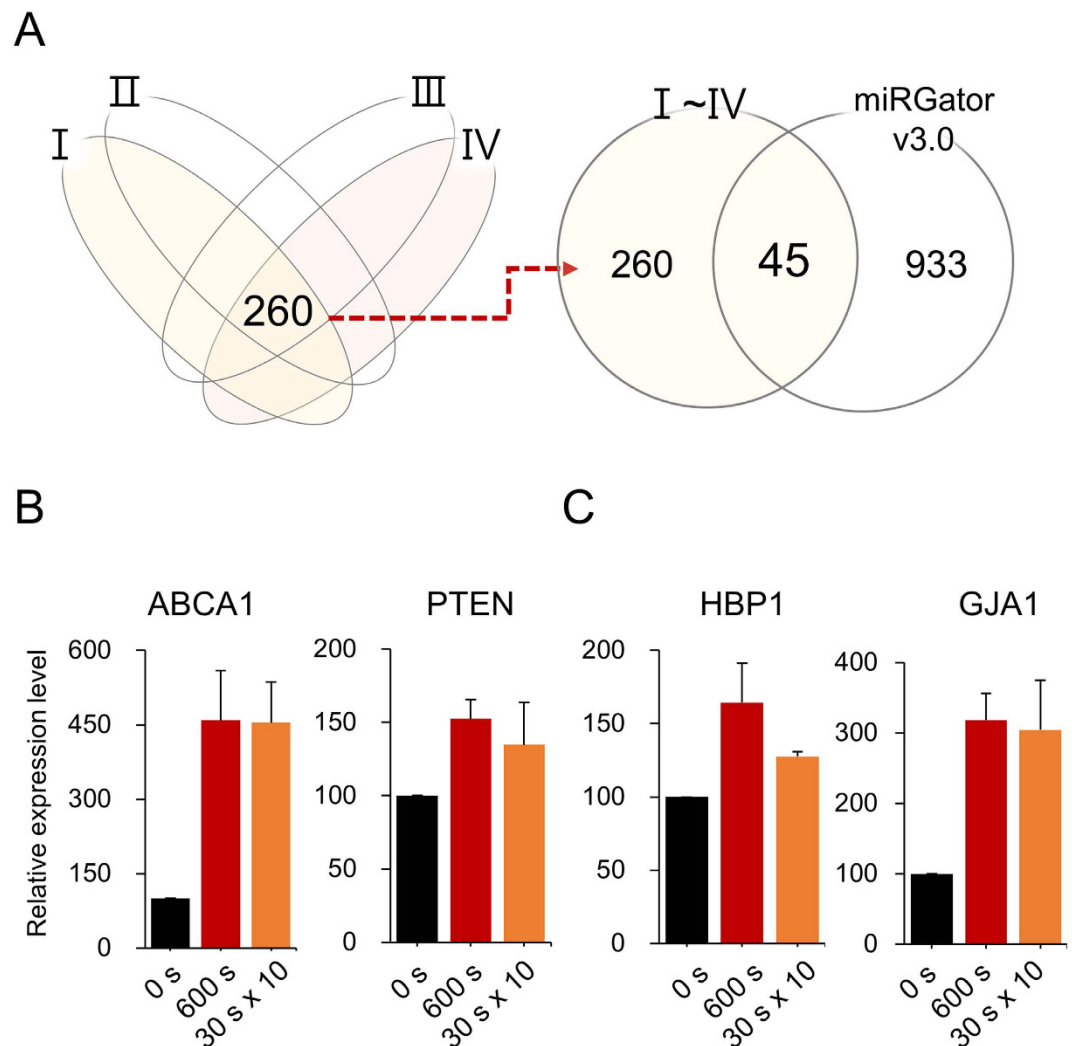


Figure 4. Upregulation of target genes of miR-19a by CAP treatment of MCF-7. (A) The strategy for selection of target genes of miR-19a. Potential targets were initially identified using four target gene prediction programs (miRWalk, miRanda, TargetScan, miRDB [I-IV]), and the resulting 260 genes were compared with miRGator to finally obtain 45 genes. (B) Upregulation of ABCA1 and PTEN, which were previously known as the target genes of miR-19a. (C) Upregulation of HBP1 and GJA1, which were newly identified as targets of miR-19a in this study. All the experiments were performed in triplicates, and the result is depicted as Mean \pm SE.

Previous studies have shown a higher rate of cell death in a variety of cancer cells than in normal cells, such as lung and melanoma cancer^{5,45,46}. This phenomenon is believed to be at least in part due to the elevated level of ROS in cancer cells, and CAP accumulates more ROS upon it, eventually leading to cell death⁴⁵. We also found downregulation of miR-19a in MDA-MB-231 other than MCF-7 (Supplementary Fig. S1), supporting the same effect of CAP on the downregulation of miR-19a in different cell types. However, more cell types should be examined to determine whether the downregulation of the miR in cancer is a general observation. It should also be mentioned that the molecular mechanism for how the signal from CAP is transduced to the alteration of miR-19a expression has yet to be elucidated. The alteration of the CpG methylation at the miR's promoter could give insight into identifying mediators in the CAP-elicited deregulation of miR-19a and its target genes.

In conclusion, this study identified that miR-19a, known as an oncomiR, underwent hypermethylation and downregulation and that the target genes of miR-19a were upregulated in the MCF-7 breast cancer cell by CAP treatment. In addition, the cell proliferation effect after the overexpression of miR-19a was suppressed by CAP. These results could contribute to establishing the epigenetic mechanism of CAP when it is applied to cells as well as tissues for cancer treatment application.

Materials and Methods

Cell culture and cold atmospheric CAP treatment of cells. The human breast cancer cell lines MCF-7 and MDA-MB-231 were purchased from the American Type Culture Collection (ATCC) (Manassas, VA, USA) and cultured in RPMI 1640 (Gibco, Los Angeles, USA) supplemented with 10% FBS (Gibco) and 2% Penicillin

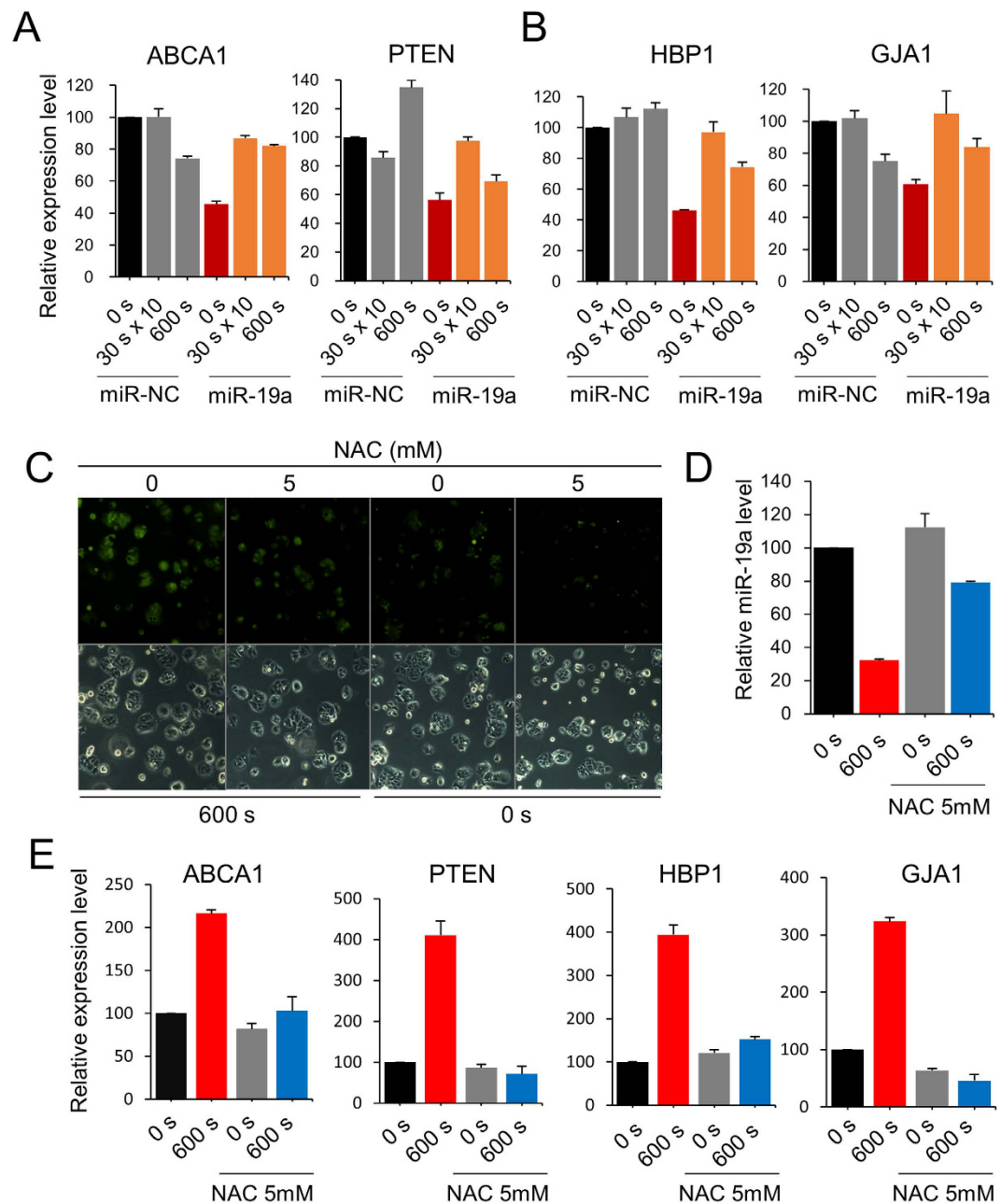


Figure 5. CAP deteriorates the downregulation effect of miR-19a on target genes. After transfection of mimic or control (NC) miR into MCF-7, the cells were treated with CAP for 600 s or 10 times for 30 s. Expression of indicated genes was examined by quantitative RT-PCR. (A) Expression of ABCA1 and PTEN, which were previously known as target genes of miR-19a. (B) Expression of HBP1 and GJA1, which were newly identified as target genes of miR-19a in this study. (C) Fluorescence microscopic images of the MCF-7 cell after treating the cell with an ROS inhibitor, N-Acetyl-L-cysteine. The bottom panel shows images from bright-field microscopy. Effect of ROS inhibitor on the expression of miR-19a (D) and target genes (E) were analyzed by quantitative RT-PCR. All the experiments were performed in triplicates, and the result is depicted as Mean \pm SE.

and Streptomycin (Gibco) under humid conditions with 5% CO₂ at 37 °C. The electrode type of the CAP device, manufactured at the Plasma Bioscience Research Center (Kwangwoon University, Korea), was mesh-DBD (Dielectric Barrier Discharge). The discharged voltage was measured at a strength of 0.46 kV when the supply voltage was set to 0.12 kV with 1.5 L/min of argon gas as a feeding gas. The chosen operational frequency was 12.89 kHz. Cells in the culture media were exposed to the CAP source ten times for 30 seconds every hour or one time for 100 sec or 600 sec.

MicroRNA transfection. MiR-19a mimic and miR-negative control (miR-NC) were synthesized by Bioneer (Korea) (Supplementary Table S2), and their sequences were based on the miRBase sequence database (<http://>

www.mirbase.org/). To perform the overexpression study of miR-19a, the miR and its negative control were transiently transfected into the cells in 50–60% confluency at 30 nM of the final concentration using Lipofectamine 2000 reagent (Invitrogen, Carlsbad, CA, USA) in serum-free Opti-MEM I Medium (Gibco). Twenty-four hours after the transfection, the cells were harvested for RNA isolation.

RNA extraction and Real-time RT-PCR. Total RNA was extracted at least twenty-four hours after CAP treatment from cells using the ZR-Duet DNA/RNA MiniPrep kit (Zymo Research, Irvine, CA, USA) following the manufacturer's protocol. To quantify the level of mature miR-19a, reverse transcription with the extracted RNA was carried out using the miScript II RT Kit (Qiagen, Valencia, CA, USA). Quantitative RT-PCR was then conducted with the miScript SYBR Green PCR Kit (Qiagen) and miScript Primer Assays as the primers. In the case of the quantification of protein-coding genes' expression level, cDNA was synthesized using ReverTra Ace qPCR RT Master Mix with gDNA remover (Toyobo, Japan), and KAPA SYBR FAST qPCR Kit Master Mix ABI Prism (Kapa Biosystems, Inc., Wilmington, MA, USA) was used for real-time PCR reaction. U6 and GAPDH were used for normalizing the expression of miR-19a and the protein-coding genes, respectively, with the $2^{-\Delta\Delta C_t}$ method. Each RT-PCR reaction was assayed in triplicate on an ABI 7300 instrument (Applied Biosystems, Foster City, CA, USA). The primers used for the amplification of miRs and selected genes are listed in Supplementary Table S2.

Cell proliferation assay. Cell growth was monitored using CCK-8 assay (Dojindo Molecular Technologies, MD, USA), which is a colorimetric assay using water-soluble tetrazolium salts that generate a yellow or orange formazan dye through interaction with viable cells. 3×10^3 cells/well of MCF-7 were seeded in 96-well plates in triplicate. Twenty-four hours after seeding, 30 nM of miR-19a mimic and control miR were transiently transfected using Lipofectamine 2000 reagent (Invitrogen) and cultured at 0, 3, and 6 days at 37 °C in a humidified environment of 5% CO₂. One-tenth of the media volume of CCK-8 reagent solution was then added into each well and incubated for two hours. The absorbance value at 450 nm (A450) was measured with a microplate reader, as was the absorbance at 600 nm (A600) as a reference. The effect of turbidity was eliminated by subtracting the A600 value from the A450 value of the same well.

Colony formation assay. 5×10^3 MCF-7 cells transfected with miR mimic or control miR in a 60-mm culture dish were maintained in a humidified atmosphere of 5% CO₂ at 37 °C for 14 days. After being fixed (methanol:acetic acid = 7:1), the colonies were stained with 0.5% crystal violet for one hour at room temperature and washed with 1xPBS (Gibco). The colonies were counted using ImageJ software (National Institutes of Health, Bethesda, MD, USA).

Extraction of differentially methylated miRs by CAP. Differentially methylated CpGs in the promoter of the non-coding RNA were extracted from previously published Illumina Infinium Human Methylation 450 K array data from NCBI's GEO dataset (GEO accession number: GSE65085) with the criteria of $|\Delta\beta| \geq 0.15$ after removing the observations with a *p*-value of ≥ 0.05 . $\Delta\beta$ was calculated by subtracting the methylation level (β value) of the non-treated cells from that of the CAP-treated cells.

Measurement of reactive oxygen species levels (ROS). The generation of ROS in cultured cells treated with CAP was quantified using the cell-permeant fluorescence probe, 2', 7'-dichlorofluorescein diacetate (DCFH-DA; Sigma-Aldrich, St Louis, MO, USA). Cells were stained with 20 μ M of DCFH-DA for 30 min at 37 °C and then exposed to CAP for 0, 100, and 600 sec. Thirty minutes after incubation at 37 °C in the dark, the fluorescence intensities of the DCFH-DA in the cells displaying intracellular ROS levels were detected by fluorescence microscopy (Leica Microsystems, Germany) and quantified using Infinite 200 Pro fluorescence reader (Tecan, Switzerland). To inhibit the production of intracellular ROS, 5 mM of N-Acetyl-L-cysteine (NAC; Sigma-Aldrich), known as a scavenger of ROS, was used to treat 5×10^5 cells in a 60-mm culture dish. After incubation for two hours, the cells were exposed to CAP and the intracellular ROS levels were measured with the aforementioned procedure.

Statistical analysis. All experimental results were plotted using Microsoft Excel software (2013 for Windows) as the mean \pm standard error of three independent experiments. Student's *t*-test was carried out for checking the statistical significance. Differences were considered statistically significant when the *p*-value was lower than 0.05.

References

- Kalghatgi, S. *et al.* Effects of non-thermal plasma on mammalian cells. *PLoS One* **6**, e16270 (2011).
- Keidar, M. *et al.* Cold plasma selectivity and the possibility of a paradigm shift in cancer therapy. *Br. J. Cancer* **105**, 1295–1301 (2011).
- Arndt, S. *et al.* Cold atmospheric plasma, a new strategy to induce senescence in melanoma cells. *Exp. Dermatol.* **22**, 284–289 (2013).
- Wang, M. *et al.* Cold atmospheric plasma for selectively ablating metastatic breast cancer cells. *PLoS One* **8**, e73741 (2013).
- Kim, S. J. & Chung, T. H. Cold atmospheric plasma jet-generated RONS and their selective effects on normal and carcinoma cells. *Sci. Rep.* **6**, 20332 (2016).
- Utsumi, F. *et al.* Effect of indirect nonequilibrium atmospheric pressure plasma on anti-proliferative activity against chronic chemo-resistant ovarian cancer cells *in vitro* and *in vivo*. *PLoS One* **8**, e81576 (2013).
- Xu, G. M. *et al.* Dual effects of atmospheric pressure plasma jet on skin wound healing of mice. *Wound Repair Regen.* **23**, 878–884 (2015).
- Ulrich, C. *et al.* Clinical use of cold atmospheric pressure argon plasma in chronic leg ulcers: A pilot study. *J. Wound Care* **24**(196), 198–200, 202–193 (2015).
- Bekeschus, S. *et al.* Hydrogen peroxide: A central player in physical plasma-induced oxidative stress in human blood cells. *Free Radic. Res.* **48**, 542–549 (2014).

10. Gupta, S. C. *et al.* Upsides and downsides of reactive oxygen species for cancer: the roles of reactive oxygen species in tumorigenesis, prevention, and therapy. *Antioxid. Redox Signal.* **16**, 1295–1322 (2012).
11. Azad, M. B., Chen, Y. & Gibson, S. B. Regulation of autophagy by reactive oxygen species (ROS): implications for cancer progression and treatment. *Antioxid. Redox Signal.* **11**, 777–790 (2009).
12. Shan, Y. *et al.* Macranthoside B Induces Apoptosis and Autophagy Via Reactive Oxygen Species Accumulation in Human Ovarian Cancer A2780 Cells. *Nutr. Cancer* **68**, 280–289 (2016).
13. Fisher, A. B. Redox signaling across cell membranes. *Antioxid. Redox Signal.* **11**, 1349–1356 (2009).
14. Zhong, S. Y. *et al.* Surface air plasma-induced cell death and cytokine release of human keratinocytes in the context of psoriasis. *Br. J. Dermatol.* **174**, 542–552 (2016).
15. Haertel, B. *et al.* Surface molecules on HaCaT keratinocytes after interaction with non-thermal atmospheric pressure plasma. *Cell Biol. Int.* **36**, 1217–1222 (2012).
16. Li, W. *et al.* Non-thermal plasma inhibits human cervical cancer HeLa cells invasiveness by suppressing the MAPK pathway and decreasing matrix metalloproteinase-9 expression. *Sci. Rep.* **6**, 19720 (2016).
17. Weiss, M. *et al.* Inhibition of Cell Growth of the Prostate Cancer Cell Model LNCaP by Cold Atmospheric Plasma. *In Vivo* **29**, 611–616 (2015).
18. Morales-Ramirez, P. *et al.* Assessing cellular DNA damage from a helium plasma needle. *Radiat. Res.* **179**, 669–673 (2013).
19. Veeck, J. & Esteller, M. Breast cancer epigenetics: from DNA methylation to microRNAs. *J. Mammary Gland Biol. Neoplasia* **15**, 5–17 (2010).
20. Bernstein, B. E., Meissner, A. & Lander, E. S. The mammalian epigenome. *Cell* **128**, 669–681 (2007).
21. Park, S. B. *et al.* Differential Epigenetic Effects of Atmospheric Cold Plasma on MCF-7 and MDA-MB-231 Breast Cancer Cells. *PLoS One* **10**, e0129931 (2015).
22. Zearo, S. *et al.* MicroRNA-484 is more highly expressed in serum of early breast cancer patients compared to healthy volunteers. *BMC Cancer* **14**, 200 (2014).
23. Shan, S. W. *et al.* Mature miR-17-5p and passenger miR-17-3p induce hepatocellular carcinoma by targeting PTEN, GalNT7 and vimentin in different signal pathways. *J. Cell Sci.* **126**, 1517–1530 (2013).
24. Nishikawa, R. *et al.* Tumor-suppressive microRNA-29s inhibit cancer cell migration and invasion via targeting LAMC1 in prostate cancer. *Int. J. Oncol.* **45**, 401–410 (2014).
25. Fu, X. *et al.* MicroRNA-103 suppresses tumor cell proliferation by targeting PDCD10 in prostate cancer. *Prostate* **76**, 543–551 (2016).
26. Hsu, T. I. *et al.* MicroRNA-18a is elevated in prostate cancer and promotes tumorigenesis through suppressing STK4 *in vitro* and *in vivo*. *Oncogenesis* **3**, e99 (2014).
27. Wu, Q. *et al.* MiR-19a/b modulate the metastasis of gastric cancer cells by targeting the tumour suppressor MXD1. *Cell Death Dis.* **5**, e1144 (2014).
28. Tan, Y. *et al.* Sp1-driven up-regulation of miR-19a decreases RHOB and promotes pancreatic cancer. *Oncotarget* **6**, 17391–17403 (2015).
29. Cho, S. *et al.* MiRGator v3.0: a microRNA portal for deep sequencing, expression profiling and mRNA targeting. *Nucleic Acids Res.* **41**, D252–257 (2013).
30. Mo, W. *et al.* Identification of novel AR-targeted microRNAs mediating androgen signalling through critical pathways to regulate cell viability in prostate cancer. *PLoS One* **8**, e56592 (2013).
31. Dou, L. *et al.* MiR-19a regulates PTEN expression to mediate glycogen synthesis in hepatocytes. *Sci. Rep.* **5**, 11602 (2015).
32. Adachi, T. *et al.* Plasma-activated medium induces A549 cell injury via a spiral apoptotic cascade involving the mitochondrial-nuclear network. *Free Radic. Biol. Med.* **79**, 28–44 (2015).
33. Ahn, H. J. *et al.* Targeting cancer cells with reactive oxygen and nitrogen species generated by atmospheric-pressure air plasma. *PLoS One* **9**, e86173 (2014).
34. Virard, F. *et al.* Cold Atmospheric Plasma Induces a Predominantly Necrotic Cell Death via the Microenvironment. *PLoS One* **10**, e0133120 (2015).
35. Hou, J. *et al.* Non-thermal plasma treatment altered gene expression profiling in non-small-cell lung cancer A549 cells. *BMC Genomics* **16**, 435 (2015).
36. Bundscherer, L. *et al.* Impact of non-thermal plasma treatment on MAPK signaling pathways of human immune cell lines. *Immunobiology* **218**, 1248–1255 (2013).
37. Kumar, N. *et al.* Induced apoptosis in melanocytes cancer cell and oxidation in biomolecules through deuterium oxide generated from atmospheric pressure non-thermal plasma jet. *Sci. Rep.* **4**, 7589 (2014).
38. Chou, J. L. *et al.* Hypermethylation of the TGF-beta target, ABCA1 is associated with poor prognosis in ovarian cancer patients. *Clin. Epigenetics* **7**, 1 (2015).
39. Singha, P. K. *et al.* TGF-beta induced TM6PAI/PMEPA1 inhibits canonical Smad signaling through R-Smad sequestration and promotes non-canonical PI3K/Akt signaling by reducing PTEN in triple negative breast cancer. *Genes Cancer* **5**, 320–336 (2014).
40. Wei, C. Y. *et al.* Expression of CDKN1A/p21 and TGFBR2 in breast cancer and their prognostic significance. *Int. J. Clin. Exp. Pathol.* **8**, 14619–14629 (2015).
41. Coomans de Brachene, A. *et al.* The expression of the tumour suppressor HBP1 is down-regulated by growth factors via the PI3K/ PKB/FOXO pathway. *Biochem. J.* **460**, 25–34 (2014).
42. Plante, I., Stewart, M. K., Barr, K., Allan, A. L. & Laird, D. W. Cx43 suppresses mammary tumor metastasis to the lung in a Cx43 mutant mouse model of human disease. *Oncogene* **30**, 1681–1692 (2011).
43. Welz, C. *et al.* Cold Atmospheric Plasma: A Promising Complementary Therapy for Squamous Head and Neck Cancer. *PLoS One* **10**, e0141827 (2015).
44. Hattori, N. *et al.* Effectiveness of plasma treatment on pancreatic cancer cells. *Int. J. Oncol.* **47**, 1655–1662 (2015).
45. Panngom, K. *et al.* Preferential killing of human lung cancer cell lines with mitochondrial dysfunction by nonthermal dielectric barrier discharge plasma. *Cell Death Dis.* **4**, e642 (2013).
46. Zucker, S. N. *et al.* Preferential induction of apoptotic cell death in melanoma cells as compared with normal keratinocytes using a non-thermal plasma torch. *Cancer Biol. Ther.* **13**, 1299–1306 (2012).
47. Cai, Z. *et al.* Optimized digital counting colonies of clonogenic assays using ImageJ software and customized macros: comparison with manual counting. *Int. J. Radiat. Biol.* **87**, 1135–1146 (2011).

Acknowledgements

This study was supported by the Science Research Center Program through the National Research Foundation of Korea (NRF) funded by the Ministry of Education, Science, and Technology (NRF- 2010-0027963).

Author Contributions

Conceived and designed the experiments: S.J.K. Performed the experiments: S.L., H.L. and S.J.K. Analyzed the data: H.B., E.H.C. and S.J.K. Wrote the paper: S.L., H.L. and S.J.K.

Additional Information

Supplementary information accompanies this paper at <http://www.nature.com/srep>

Competing financial interests: The authors declare no competing financial interests.

How to cite this article: Lee, S. *et al.* Epigenetic silencing of miR-19a-3p by cold atmospheric plasma contributes to proliferation inhibition of the MCF-7 breast cancer cell. *Sci. Rep.* **6**, 30005; doi: 10.1038/srep30005 (2016).



This work is licensed under a Creative Commons Attribution 4.0 International License. The images or other third party material in this article are included in the article's Creative Commons license, unless indicated otherwise in the credit line; if the material is not included under the Creative Commons license, users will need to obtain permission from the license holder to reproduce the material. To view a copy of this license, visit <http://creativecommons.org/licenses/by/4.0/>